

Excess Gibbs Energy of Microcline-Low Albite Alkali Feldspars at 800°C and 1 Bar, Based on Fused Alkali Bromide Ion-Exchange Experiments

FRANÇOIS DELBOVE

*C.N.R.S. Centre de Recherches sur la Synthèse et la Chimie des Minéraux
45045 Orleans-Cedex, France*

Abstract

An alkali ion-exchange equilibrium curve between molten Na-K bromide and highly-ordered alkali feldspar was determined at 800°C and 1 bar. The miscibility gap in the feldspar crystalline solution occurs between $N_{Or} = 0.105$ and $N_{Or} = 0.50$ at a salt composition $M_{KBr} = 0.32$ (mole fractions). A thermodynamic analysis of combined ion-exchange and two-feldspar data yields the excess Gibbs energy of mixing of the solution with a maximum value of 900 cal mol⁻¹. This is not very different from that for high albite-sanidine feldspars, but is more accentuated in asymmetry towards NaAlSi₃O₈. Such asymmetry of \bar{G}_T^{ex} is most likely related to the excess entropy of mixing.

Introduction

Values of molar excess Gibbs energy, \bar{G}^{ex} , of mineral crystalline solutions are very much needed by petrologists, especially when dealing with phase equilibria. Such values for the mixing properties of alkali feldspars are of particular interest because these minerals frequently occur in many common terrestrial rocks.

In a previous paper (Delbove, 1971), the excess Gibbs energy of disordered synthetic alkali feldspars (high albite-sanidine) at 800°C and 1 bar was derived using the fused salt alkali-ion exchange technique of preparing feldspars of intermediate compositions and a graphical thermodynamic treatment of the ion-exchange data.

Derivation of such a quantity for highly-ordered feldspars is also of interest. Although the differences in \bar{G}^{ex} for both structural types of feldspars are relatively small as compared with the ideal mixing Gibbs energy, the differences have a substantial effect on the feldspar phase relations.

Bachinski and Müller (1971) provide a good review of previous work on this subject. The current status of the alkali feldspars is as follows: at one atmosphere and at a high enough temperature, the subsolidus region of this binary system is characterized by a continuous crystalline solution series. With decreasing temperature, the greater influence of a positive excess Gibbs energy results in unmixing with separation of Ab-rich and Or-rich phases. Recent studies have

shown the influence of structural order on the solvus, the most recent indication being that the solvus for the ordered series is outside that for the disordered one. For example, at 800°C and 1 bar, complete solid solution exists between sanidine and high albite (Orville, 1963; Thompson and Waldbaum, 1969b; Delbove, 1971), whereas a miscibility gap exists between microcline and low albite (Bachinski and Müller, 1971).

The fused salt technique is the only one that permits work at one atmosphere, and it is the only one which provides exchanged products structurally unmodified as to the Al-Si occupancy of the $T(O)$ and $T(m)$ sites. However, the occurrence of a miscibility gap requires a modification of the previous thermodynamic treatment (Delbove, 1971).

Experimental Details

Starting Materials

The natural microcline used as a starting material was a portion of a decimeter-sized perthite crystal from an intrusive pegmatite in Precambrian gneiss of southern Norway (exact location of this feldspar is not known) and was supplied to us by Pr. Dr. G. Sabatier. The microcline has well developed grid-twinning. Albite included within the microcline occurs in small optically continuous patches and in apparent crystallographic continuity with the microcline host. The albite inclusions show polysynthetic albite-twinning. The bulk composition

TABLE 1. Composition of Natural Starting Alkali Feldspar

Oxide	Weight Percent	Feldspar	Mole Percent
SiO ₂	64.40	NaAlSi ₃ O ₈	16.8
Al ₂ O ₃	18.50	KAlSi ₃ O ₈	81.5
TiO ₂	0.09		
Fe ₂ O ₃	0.22	RbAlSi ₃ O ₈	0.35
Na ₂ O	1.93	CaAl ₂ Si ₂ O ₈	1.35
K ₂ O	14.25		
Rb ₂ O	0.13		
CaO	0.28		
Total	99.80		

of the microcline starting material, as determined by chemical analysis (see Table 1), is Or_{81.50}Ab_{18.8}An_{1.3}Rb-feldspar_{0.4} (mole percent). The influence of the An-content and that of Rb-feldspar will be neglected and the feldspar treated as a simple binary Na-K solution.

From X-ray examination (see Tables 2 and 3) the compositions of the two perthitic phases are estimated to be Or₁ and Or₉₈ mole percent, which, according to the middle solvus reported in Figure 9 of Bachinski and Müller (1971), indicates a temperature of formation of about 380°C.

Ion-Exchange Procedures

The natural microcline starting material was finely crushed and sieved, with subsequent procedures being carried out on the 100–200 mesh fraction. The experiments were performed using the latter material (about 100 mg for each run) and thoroughly dried alkali bromide of various Na,K ratios. For all runs the relative alkali molar proportions of the system: feldspar + salt were set to be roughly similar, *i.e.* [(Na + K)felds/(Na + K)salt] ≈ 1:3, in order to ensure good contact between the exchanging phases. The exact proportions are given in Table 3 for each run. These materials were sealed together in platinum capsules and placed at one atmosphere pressure in a vertical-bore quenching furnace regulated at 800 ± 5°C with a Ni-Cr/Ni-Al thermocouple. After a variable period, ranging from 6 to 31 days, the capsules were quenched to room temperature by allowing them to fall into a container of water under the furnace.

After opening of the capsules, the salt was separated from feldspar by dissolution in distilled water, followed by determination of the Na and K constituents by flame-photometric analysis. The feldspar, after drying, was examined by X-ray diffraction in order to detect any possible new phases or change of structural state, and its Or-content determined using the $\bar{2}01$ method of Orville (1967). A question

TABLE 2. Cell Parameters and Related Structural Data for Alkali Exchanged Feldspars of This Study

Run No.	Cell Volume (Å ³)	N _{Or} (mol%)	a (Å)	(a)	b (Å)	c (Å)	α (deg.)	β (deg.)	γ (deg.)	α* (deg.)	γ* (deg.)	Δ (b°)	Δ (α*γ*)	Tr [110] (Å)	Tr [110] (Å)
St. Fe1.	721.00 0.25	92.5	8.5656 0.0015	(8.61)	12.9682 0.0011	7.2232 0.0010	90.632 0.011	115.921 0.009	87.628 0.010	90.450 0.011	92.330 0.009	0.995	0.980	15.834	15.243
2-4*	664.73 0.22	2.5	8.1402 0.0017	(8.15)	12.7920 0.0016	7.1602 0.0009	94.258 0.012	116.614 0.009	87.706 0.013	86.385 0.011	90.538 0.012	0.985	0.980	15.435	14.885
5-5	667.58 0.38	5.5	8.1612 0.0026	(8.16)	12.7995 0.0026	7.1628 0.0017	94.003 0.025	116.563 0.017	87.731 0.026	86.658 0.020	90.538 0.021	0.980	0.970	15.450	14.905
6-6	667.70 0.37	6.0	8.1627 0.0024	(8.16)	12.8056 0.0033	7.1591 0.0017	93.973 0.026	116.562 0.016	87.718 0.024	86.697 0.021	90.567 0.019	0.945	0.970	15.458	14.909
9-6	668.95 0.34	7.0	8.1727 0.0024	(8.17)	12.8077 0.0021	7.1606 0.0015	93.910 0.022	116.539 0.014	87.744 0.020	86.755 0.019	90.571 0.016	0.950	0.970	15.462	14.919
4-4	671.16 0.47	10.0	8.1866 0.0030	(8.18)	12.8235 0.0024	7.1631 0.0020	93.717 0.024	116.562 0.018	87.763 0.024	86.961 0.021	90.644 0.021	0.930	0.960	15.481	14.942
2-5	708.14 0.31	63.0	8.4361 0.0019	(8.48)	12.9520 0.0015	7.2111 0.0014	91.114 0.015	115.897 0.012	87.546 0.016	89.952 0.012	92.187 0.014	0.955	1.060	15.757	15.151
4-7*	707.44 0.56	62.0	8.4410 0.0033	(8.46)	12.9458 0.0019	7.2101 0.0022	91.177 0.031	116.019 0.021	87.663 0.027	89.830 0.026	92.026 0.022	0.965	1.020	15.740	15.164
1-4	708.92 0.16	65.0	8.4473 0.0011	(8.48)	12.9508 0.0008	7.2113 0.0007	91.037 0.009	115.921 0.005	87.587 0.010	90.019 0.007	92.179 0.008	0.965	1.040	15.757	15.162
4-1	715.76 0.32	79.0	8.5127 0.0020	(8.56)	12.9617 0.0014	7.2183 0.0016	90.939 0.020	115.903 0.014	87.501 0.020	90.169 0.015	92.322 0.015	0.980	1.080	15.814	15.194
1-8*	720.08 0.29	90.0	8.5611 0.0019	(8.56)	12.9649 0.0012	7.2157 0.0016	90.682 0.019	115.681 0.015	87.663 0.017	90.375 0.015	92.267 0.013	0.955	1.010	15.825	15.242
4-8	720.50 0.18	91.0	8.5631 0.0012	(8.58)	12.9647 0.0008	7.2220 0.0008	90.670 0.008	115.918 0.006	87.631 0.007	90.407 0.007	92.309 0.006	0.995	1.030	15.830	15.239
2-8*	721.83 0.30	95.0	8.5772 0.0020	(8.60)	12.9667 0.0017	7.2221 0.0012	90.661 0.019	115.915 0.011	87.640 0.017	90.412 0.015	92.303 0.013	0.990	1.030	15.839	15.249
1-6	722.75 0.17	97.5	8.5906 0.0010	(8.58)	12.9664 0.0007	7.2210 0.0008	90.623 0.008	115.929 0.007	87.659 0.007	90.446 0.008	92.300 0.007	0.985	1.020	15.844	15.259

(a) indicates the expected value of a (angstroms) estimated from the contours on the revised b-a plot of Stewart and Wright (1974).

Numbers of runs with an asterisk refer to runs starting with Na-exchanged feldspar.

St. Fe1. refers to the natural perthitic starting feldspar (only its microcline part is described here).

Run 4-4 results in a nearly quite albitic perthitic feldspar (Or-peaks are too weak to permit a least-squares refinement).

TABLE 3. Alkali Feldspar Molten Alkali Bromide Ion-Exchange Data

Run No.	Time (days)	Salt Mole Frac	$2\theta(\bar{2}01)$ (deg)	N_{Or} (mol%)	Cell Volume (\AA^3)	N_{Or} (mol%)	M_{KBr} (mol%)	$Z(N_{Or})$ (cal/mol)
St. Fel.			22.040	1.0				
--			21.035	94.0	721.000	92.5		
2-4*	31	0.740	22.035	1.5	664.734	2.5	5.5	2860 (1750)
8-6	19	0.815	22.000	4.0			15.0	3080
1-7*	26	0.805	21.990	5.0			22.0	3580
5-5	25	0.740	21.980	6.0	667.575	5.5	24.0	3410 (3600)
6-6	19	0.795	21.980	6.0	667.700	6.0	25.0	3520 (3520)
7-6	19	0.750	21.970	6.5			21.0	2860
1-1	12	0.740	21.965	7.0			24.0	3060
2-7*	26	0.810	21.970	6.5			26.5	3510
9-6	19	0.715	21.960	7.5	668.953	7.0	28.0	3340 (3500)
4-4	31	0.830	21.925	10.5	671.157	10.0	32.0	2960 (3080)
--			21.490	45.0				-1180
3-5	25	0.755	21.910	11.5			32.0	2740
--			21.440	50.5				-1650
4-5	25	0.800	21.925	10.5			31.5	2910
--			21.460	48.0				-1490
3-7*	26	0.800	21.930	10.0			33.0	3170
--			21.420	52.5				-1720
2-5	25	0.810	21.340	61.5	708.140	63.0	36.0	-2220 (-2360)
4-7*	26	0.805	21.335	62.0	707.441	62.0	37.0	-2180 (-2180)
1-4	31	0.830	21.320	63.5	708.925	65.0	38.0	-2220 (-2360)
4-1	12	0.750	21.170	79.5	715.757	79.0	48.5	-3020 (-2950)
1-5	25	0.805	21.145	82.5			53.0	-3050
4-6	19	0.815	21.135	83.5			51.5	-3330
3-6	19	0.765	21.120	85.0			60.5	-2790
5-1	12	0.710	21.080	89.5			70.5	-2710
5-4	31	0.805	21.070	90.5			61.0	-3850
1-8*	7	0.825	21.060	91.5	720.078	90.0	65.0	-3750 (-3360)
5-7*	26	0.820	21.060	91.5			66.5	-3600
4-8	7	0.790	21.050	92.5	720.496	91.0	61.5	-4360 (-3930)
2-6	19	0.770	21.050	92.5			76.0	-2900
3-8	7	0.780	21.030	91.5			81.0	-2970
2-8*	7	0.835	21.030	94.5	721.830	95.0	82.0	-2830 (-3040)
1-6	19	0.790	21.000	97.5	722.749	97.5	95.0	-1530 (-1530)

Values in the third column refer to the bulk composition of the runs expressed as mole fraction salt/(salt + feldspar).

Values of N_{Or} in the fifth column are deduced from $2\theta(\bar{2}01)$.

Values of N_{Or} in the seventh column are deduced from cell volumes (see Table 2).

Values of Z in parentheses in the last column are calculated with the latter values of N_{Or} .

arose as to the validity of the latter method for determining the composition of alkali feldspars. As shown by Wright and Stewart (1968), this method is practical only in the case of feldspars for which the structural state is well-defined and not "anomalous." Consideration of the X-ray diffraction data in more detail is therefore necessary.

X-ray Diffraction Data

The X-ray data of this study were obtained with a C. G. R. diffractometer with Ni-filtered copper radiation. Scans were made at $1/5^\circ 2\theta$ per minute, and a time constant of 10 seconds. The diffractometer was operated with a Geiger sensing element, 1.15° scatter and divergence slits, 0.01 inch receiving slit ($0.065^\circ 2\theta$). The X-ray wavelength used for $\text{CuK}\alpha_1$, $1.540562 \pm 0.000007 \text{ \AA}$, is from Bearden (1967).

Each sample was mixed with reagent-grade KBrO_3 (from Prolabo, France) used as an internal standard. Two forward and reverse scans were made in the range 19 to 23 degrees 2θ . The composition of the

alkali feldspar (in mole percent Or) was deduced from the difference in 2θ between the $\bar{2}01$ reflection of the feldspar and the 101 reflection of KBrO_3 , using the determinative $\Delta(2\theta)$ curve of Orville (1967, Fig. 8) for the microcline-low albite series. Results of these determinations are given in Table 3, with corresponding values of $\Delta(2\theta)$ being converted to $2\theta \bar{2}01$, using $2\theta 101$ equal to 20.212° , as given by Orville (p. 75).

However, these determinations are somewhat uncertain, due to some possible anomalies of the cell dimensions of our feldspars, and these are, perhaps, not as highly ordered as were the feldspars Orville used to plot his $\Delta(2\theta)$ curve. So, a determination of cell-parameters seemed highly desirable.

This was performed on some of the samples, using semi-conductor grade silicon (99.999 from Koch-Light, England) as an internal standard. The value of $a = 5.43093 \pm 0.00008 \text{ \AA}$ was taken for this Si. Two forward and reverse scans were made in the range 20 to 60 degrees 2θ . Only the lines that could be indexed unambiguously were taken into account and their positions measured using the absolute 2θ values, 28.442° , 47.302° , and 56.122° for the three standard Si peaks covering the 2θ range. It was confirmed, on such an occasion, that $2\theta(\bar{2}01)$ values measured in this way agreed within less than $0.020^\circ 2\theta$ with those previously measured using KBrO_3 .

Unit-cell parameters were then determined by least-squares refinement using the digital computer program LCLSQ of Burnham (1962), slightly modified and kindly provided to us by D. R. Waldbaum. Results of these refinements are given in Table 2; the uncertainties reported in the cell parameters are least-squares standard errors as defined by Burnham.

To obtain an evaluation of the degree of order, we shall first consider the variations of the b , c and α^* , γ^* cell parameters. These values are plotted in Figures 1 and 2 together with the $b - c$ and $\alpha^* - \gamma^*$ quadrilaterals obtained by connecting the preferred end-member values of Stewart and Wright (1974) by straight lines. Individual data points of this study may be seen to be near the microcline-low albite sides. The values of $\Delta(bc)$ and $\Delta(\alpha^*\gamma^*)$, as defined by Stewart and Ribbe (1969), are also reported in Table 2: they are very near the limiting theoretical value of 1 for highly-ordered alkali feldspars, except in the 60-90 mole percent Or composition range, where the value of $\Delta(\alpha^*\gamma^*)$ exceeds 1 by more than 0.05. These values indicate, according to Stewart and Ribbe, an Al-occupancy of T_1O sites, t_{10} , nearly equal to 1, whereas T_1m , T_2O , and T_2m would be nearly Al-

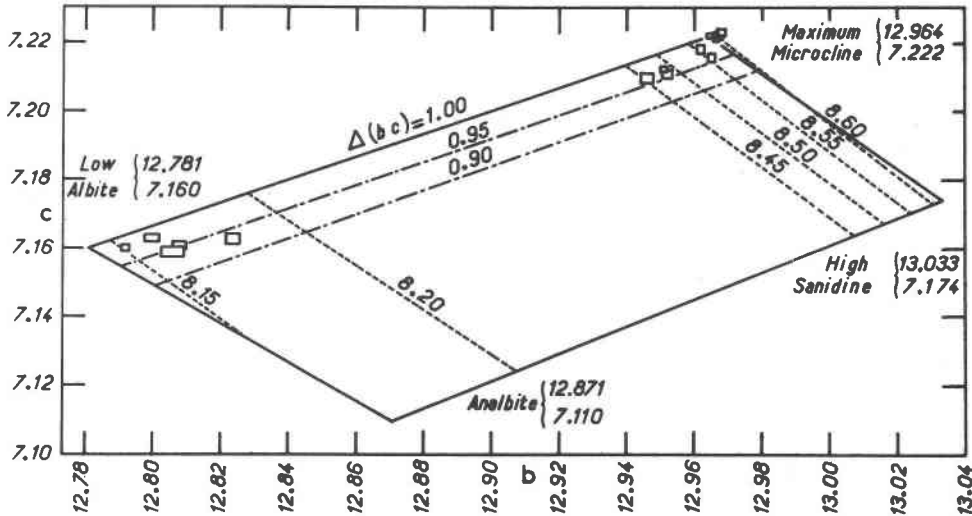


FIG. 1. *b* plotted against *c* for alkali exchanged feldspars; data from Table 2, this paper. Cell data points are drawn to ± 1 standard deviation of the cell parameters. Solid lines connect preferred limiting reference values of Stewart and Wright (1974). Dashed lines are contours for the *a* axis, and dot-dashed lines equal $\Delta(bc)$ lines from the same authors.

free ($t_{1m} \approx t_{20} \approx t_{2m} \approx 0$). Contours plotted for the *a* axis in Figure 2 are also from Stewart and Wright (1974); refined values of *a* do not differ from the expected ones by more than 0.05 Å.

Another method for estimating the Al,Si distribution in alkali feldspars is the one described by Kroll (1973) who considers the translational distances in the [110] and $[1\bar{1}0]$ directions, namely Tr [110] and Tr $[1\bar{1}0]$. These distances, which can be calculated from the *a*, *b*, and γ refined unit-cell parameters, are also reported in Table 2 and plotted in Figure 3 against compositions (these being determined from cell-volumes, as will be indicated later). The smooth curves represented in the figure connect the values calculated by Kroll (1973, Fig. 5) for the low albite-microcline series (with the hypothesis: $t_{10} = 0.87$, $t_{1m} = t_{20} = t_{2m} = 0.04$) and for the high albite-sanidine series (with the hypothesis: $t_{10} = t_{1m} = t_{20} = t_{2m} = 0.25$). The slight departure of Tr [110] and Tr $[1\bar{1}0]$ point data from the smooth curves relative to the low albite-microcline series may be an indication of t_{10} being greater than 0.87 and of t_{1m} , t_{20} , and t_{2m} being less than 0.04 in our feldspars.

In order to test the compositions previously determined using the positions of $2\theta(201)$ X-ray peaks, we have redetermined them using refined unit-cell volumes. An available equation relating molar volumes to compositions is that of Waldbaum and Robie (1971, p. 394): $\bar{V} = 2.38497 + 0.21962 N_{Or} + 0.1096 N_{Or} \cdot N_{Ab}$ cal bar $^{-1}$ mol $^{-1}$. Converting cal bar $^{-1}$

mol $^{-1}$ to Å 3 , with a value of $N_{Av} = 6.0247 \cdot 10^{23}$ and a unit-cell containing 4 "molecules" of feldspar, gives: v (in Å 3) = 662.520 + 61.002 N_{Or} + 30.448 $N_{Or} N_{Ab}$. N_{Or} values so determined (Table 3) may be seen to differ by less than 2 percent from those previously determined using $\bar{2}01$. So, we may conclude that the

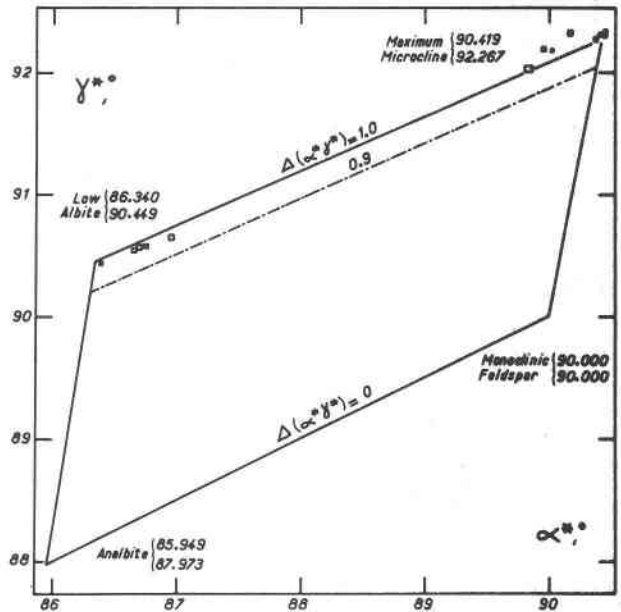


FIG. 2. α^* plotted against γ^* for alkali exchanged feldspars; data from Table 2, this paper. Cell data points are drawn to ± 1 standard deviation of the cell parameters. Solid lines connect preferred limiting reference values of Stewart and Wright (1974). Dot-dashed lines are equal $\Delta(\alpha^* \gamma^*)$ lines from the same authors.

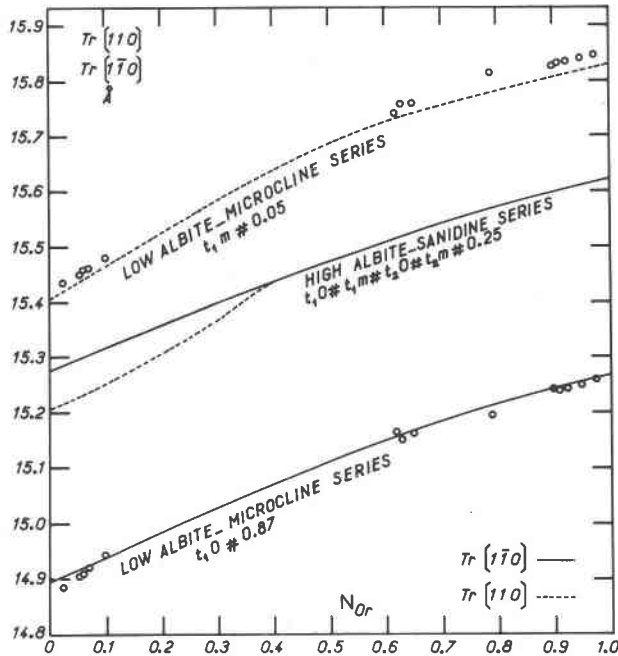


FIG. 3. $Tr [110]$ and $Tr [1\bar{1}0]$ plotted against N_{Or} for alkali-exchanged feldspars; data from Table 2, this paper. The solid $Tr [1\bar{1}0]$ and dashed $Tr [110]$ curves are drawn using values for both extreme feldspar series as plotted in Figure 5 of Kroll (1973), with site occupancies as indicated by Kroll in abscissa.

201 method is reliable when applied to feldspars of this study.

Experimental Results

The ion-exchange equilibrium data are summarized in Table 3, where feldspar and salt compositions are expressed as mole percent orthoclase [$N_{Or} = 100 \text{ KAlSi}_3\text{O}_8 / (\text{NaAlSi}_3\text{O}_8 + \text{KAlSi}_3\text{O}_8)$] and as mole percent KBr [$M_{KBr} = 100 \text{ KBr} / (\text{NaBr} + \text{KBr})$]. These compositions, expressed as mole fractions, are also plotted as ordinate and abscissa in Figure 4.

Almost all the run products consist of single-phase feldspar, as evidenced by a single sharp 201 X-ray diffraction peak, although the starting feldspar was a two-phase mixture. Measured N_{Or} compositions give a distribution of data which extend from 0 to 10, and 50 to 100 mole percent Or. Some runs (4-4, 3-5, 4-5, and 3-7), however, give an evidence of a two-phase feldspar. The X-ray data for these latter runs indicate feldspar compositions to be 10 ± 1 and 50 ± 2 mole percent Or. The corresponding composition of the salt phase is 32 ± 0.5 mole percent KBr.

The curve of Figure 4 may be considered as a graphical description of equilibrium exchange relations between ordered alkali feldspar and fused $(\text{Na},\text{K})\text{Br}$ at 800°C and 1 bar, with the dotted vertical

line denoting the solvus compositions $N_{Or,I} = 0.10$, $N_{Or,II} = 0.50$ to be in invariant isothermal isobaric equilibrium with molten salt composition $M_{KBr,I-II} = 0.32$.

On considering these results, it is essential to wonder first whether exchange equilibrium has actually been attained, a condition which is essential for the validity of the next treatment. As in our previous work (Delbove, 1971), assurance of the reversibility of data (and, hence, a check on equilibrium) was achieved through runs yielding the same feldspar compositions from opposite directions, that is, involving previously Na-exchanged as well as natural perthitic feldspar as starting feldspar materials, both giving final results on the same exchange curve. Runs starting with Na-feldspar are denoted by an asterisk in Tables 2 and 3, and by a square in Figure 4.

Second, it is essential to ensure that the compositions of the phases produced in the above-cited runs are true binodal ones, that is, that complete thermodynamic equilibrium was attained between the two feldspar phases (the reason for this requirement will be shown later in the thermodynamic treatment of the data). Such complete equilibrium is verified by the intensity of the two 201 X-ray peaks being variable in relative magnitude with respect to each

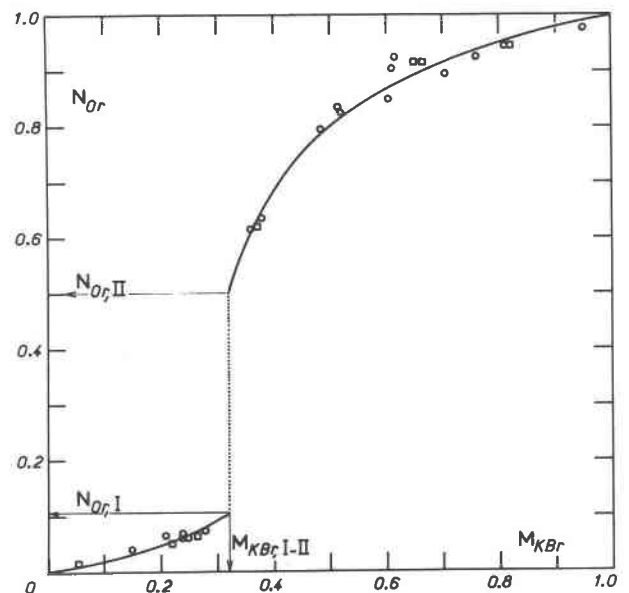


FIG. 4. Alkali distribution curve at 800°C and 1 bar between fused alkali bromide and highly-ordered alkali feldspar; data from Table 3, this paper. Open circles represent runs starting with natural original perthitic feldspar, open squares runs with the same but previously Na-exchanged feldspar. The vertical dotted line represents the miscibility gap in the feldspar crystalline solution at this temperature and this pressure.

other. This results from the variable relative ratios of each perthitic feldspar in the exchange products, one feldspar phase being able to develop at the expense of the other. Had each phase of the original perthite participated only in exchange equilibrium, the proportions of each perthitic feldspar phase would remain constant and, therefore, the two $\bar{2}01$ X-ray peaks would have constant magnitudes relative to each other.

Thermodynamic Analysis

Thermodynamic Definitions and Relations

The chemical potential, μ_a , of a component a , in a binary phase, ϕ , may be expressed as follows:

$$\mu_a = \mu_a^{\text{id}} + \mu_a^{\text{ex}} = G_a^\circ + RT \ln N_a + \mu_a^{\text{ex}} \quad (1)$$

where \bar{G}_a° is standard molar Gibbs energy of pure a , N_a is mole fraction of a , and μ_a^{ex} is excess chemical potential of a . The second component of ϕ , b , mole fraction $N_b = 1 - N_a$, is expressed similarly:

$$\mu_b = \mu_b^{\text{id}} + \mu_b^{\text{ex}} = G_b^\circ + RT \ln (1 - N_a) + \mu_b^{\text{ex}} \quad (1')$$

The total molar Gibbs energy of the whole phase is then given by:

$$\bar{G}_\phi = \bar{G}_\phi^{\text{id}} + \bar{G}_\phi^{\text{ex}} = N_a[G_a^\circ + RT \ln N_a + \mu_a^{\text{ex}}] + (1 - N_a)[G_b^\circ + RT \ln (1 - N_a) + \mu_b^{\text{ex}}] \quad (2)$$

By definition, the molar excess Gibbs energy, \bar{G}_ϕ^{ex} , is zero at both limiting compositions $N_a = 0$ and $N_a = 1$.

A useful classical relation for such a binary phase is:

$$(\mu_a - \mu_b)_\phi = \left[\frac{\partial \bar{G}_\phi}{\partial N_a} \right]_{P,T} \quad (3)$$

Substituting Equation (2) into Equation (3) gives:

$$(\mu_a - \mu_b)_\phi = \left[\frac{\partial \bar{G}_\phi^{\text{id}}}{\partial N_a} \right] + \left[\frac{\partial \bar{G}_\phi^{\text{ex}}}{\partial N_a} \right] \quad (4)$$

where:

$$\left[\frac{\partial \bar{G}_\phi^{\text{id}}}{\partial N_a} \right] = (G_a^\circ - G_b^\circ) + RT \log \frac{N_a}{1 - N_a} \quad (5)$$

$$\text{and:} \quad \left[\frac{\partial \bar{G}_\phi^{\text{ex}}}{\partial N_a} \right] = (\mu_a^{\text{ex}} - \mu_b^{\text{ex}})_\phi \quad (6)$$

In this study, the phases will be denoted by the subscripts f for feldspar and s for fused alkali salt, and the components by the subscripts Or, Ab, KBr, and NaBr. Compositions of each binary phase will be ex-

pressed as mole fractions N_{Or} or M_{KBr} , respectively. The two-feldspar assemblage will be characterized by the mole fractions $N_{\text{Or,I}}$ and $N_{\text{Or,II}}$, the corresponding invariant composition of fused salt being denoted $M_{\text{KBr,I-II}}$.

Basic Equilibrium Equation

Writing the alkali ion exchange reaction between feldspar and fused salt as follows:



the condition for equilibrium is given by

$$(\mu_{\text{Or}} - \mu_{\text{Ab}})_f = (\mu_{\text{KBr}} - \mu_{\text{NaBr}})_s \quad (8)$$

in terms of chemical potentials, or, according to Equation (3), by

$$\left[\frac{\partial \bar{G}_f(N_{\text{Or}})}{\partial N_{\text{Or}}} \right]_{P,T} = \left[\frac{\partial \bar{G}_s(M_{\text{KBr}})}{\partial M_{\text{KBr}}} \right]_{P,T} \quad (9)$$

in terms of total Gibbs energy.

The latter expression means that, at equilibrium compositions, slopes of tangents to both \bar{G} curves, \bar{G}_f and \bar{G}_s , are equal (see Fig. 1a of Thompson and Waldbaum, 1968).

Taking into account the relations of Equations (1) and (1'), we obtain for Equation (8)

$$(\mu_{\text{Or}}^{\text{ex}} - \mu_{\text{Ab}}^{\text{ex}})_f = -[(G_{\text{Or}}^\circ - G_{\text{Ab}}^\circ) - (G_{\text{KBr}}^\circ - G_{\text{NaBr}}^\circ)] - RT \ln \left[\frac{N_{\text{Or}} M_{\text{NaBr}}}{N_{\text{Ab}} M_{\text{KBr}}} \right] + [\mu_{\text{KBr}}^{\text{ex}} - \mu_{\text{NaBr}}^{\text{ex}}]_s \quad (10)$$

in terms of excess chemical potentials, the corresponding equation in terms of excess Gibbs energies being

$$\frac{\partial \bar{G}_f^{\text{ex}}(N_{\text{Or}})}{\partial N_{\text{Or}}} = -[(G_{\text{Or}}^\circ - G_{\text{Ab}}^\circ) - (G_{\text{KBr}}^\circ - G_{\text{NaBr}}^\circ)] - RT \ln \left[\frac{N_{\text{Or}} M_{\text{NaBr}}}{N_{\text{Ab}} M_{\text{KBr}}} \right] + \frac{\partial \bar{G}_s^{\text{ex}}(M_{\text{KBr}})}{\partial M_{\text{KBr}}} \quad (11)$$

The first bracketed quantity on the right-hand side of Equation (11) at a given temperature and pressure is a sum of constant terms; it may be expressed as a constant C :

$$C \equiv [(G_{\text{Or}}^\circ - G_{\text{Ab}}^\circ) - (G_{\text{KBr}}^\circ - G_{\text{NaBr}}^\circ)] \quad (12)$$

For the equilibrium attained, the mole fractions in the logarithm are related to one another through the exchange curve of Figure 4. Hence, this expression may be identified as the quantity Z , which is a function of any one of the mole fractions, say N_{Or} :

$$Z(N_{\text{Or}}) \equiv -RT \ln \left[\frac{N_{\text{Or}}(1 - M_{\text{KBr}})}{(1 - N_{\text{Or}})M_{\text{KBr}}} \right] \quad (13)$$

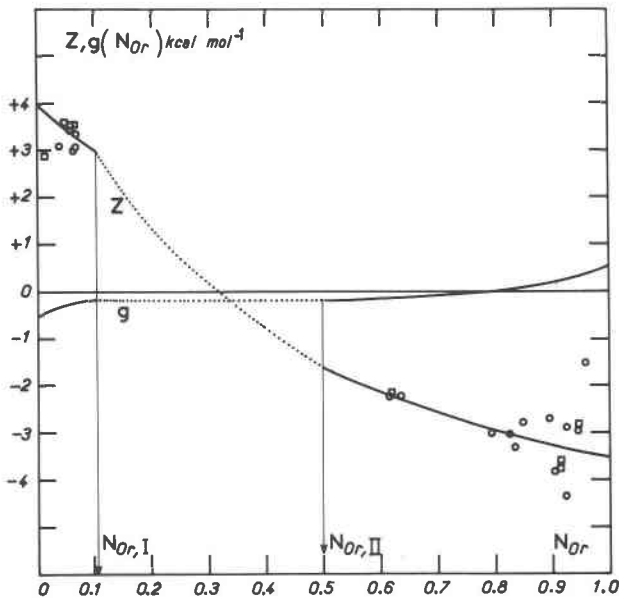


FIG. 5. Plots of

$$Z \equiv -RT \ln \left[\frac{N_{Or}(1 - M_{KBr})}{(1 - N_{Or})M_{KBr}} \right] \text{ and } g = \frac{\partial \bar{G}_s^{\text{ex}}(M_{KBr})}{\partial M_{KBr}}$$

versus N_{Or} , where N_{Or} is related to M_{KBr} through the alkali distribution curve in Figure 4. Open circles and open squares have the same signification as in Figure 4. The dotted central portions of both curves are drawn with N_{Or} assumed to vary continuously from $N_{Or,I}$ to $N_{Or,II}$ in the two-feldspar region, and M_{KBr} to be constant and equal to $M_{KBr,I-II}$.

Figure 5 shows the plot of Z against N_{Or} , where both extreme portions of the solid curve correspond to the two branches of the ion-exchange curve of Figure 4 and where the intermediate dotted portion corresponds to the vertical dotted branch. This dotted portion of Z has been calculated by setting M_{KBr} constant with the value $M_{KBr,I-II} = 0.32$ and by varying N_{Or} continuously from $N_{Or,I} = 0.105$ to $N_{Or,II} = 0.50$; the slope of this dotted portion shows a discontinuity at both junctions with the solid portion. The reason for this discontinuity is explained in Appendix B.

As for the last term in Equation (11), which refers to the molten salt, it may be expressed as a function of N_{Or} or M_{KBr} for the same reasons as above for Z , and we shall write for convenience:

$$g(N_{Or}) = \frac{\partial \bar{G}_s^{\text{ex}}(M_{KBr})}{\partial M_{KBr}} \quad (14)$$

The only available information concerning \bar{G}_s^{ex} is from the work of Hersh and Kleppa (1965) who give for the excess enthalpy of mixing of molten Na-K bromide at 770°C:

$$\bar{H}_s^{\text{ex}} = M_{NaBr}M_{KBr}[(-510) - 60M_{NaBr}] \quad (15)$$

According to the modified conformal solution theory

for molten salts of Reiss, Katz, and Kleppa (1962), only two parameters are needed to describe \bar{H}_s^{ex} to account for random mixing of Na-K cations in the molten cationic sublattice when the configurational excess entropy is assumed to be zero. Recent studies of Guion *et al* (1968) on ternary molten salt system NaCl-KCl-AgCl reveal \bar{G}^{ex} of the binary system NaCl-KCl to be -90 cal mol^{-1} at 50-50 composition, compared with a value of $-130 \text{ cal mol}^{-1}$, as given for \bar{H}^{ex} by Hersh and Kleppa (1965). Thus, the excess entropy, \bar{S}^{ex} , of this binary system is less than $-0.04 \text{ cal deg}^{-1}$ (see Waldbaum, 1969, for a more complete discussion). Due to lack of supplementary data, we have supposed \bar{S}^{ex} of the liquids in the system NaBr-KBr to be equal to zero. Thus, values of \bar{H}^{ex} calculated at 770°C for this system from Equation (15) are assumed to be relevant at 800°C. The differentiation of Equation (15) gives then:

$$\frac{\partial \bar{G}_s^{\text{ex}}(M_{KBr})}{\partial M_{KBr}} = -570 + 1260M_{KBr} - 180M_{KBr}^2 \text{ cal mol}^{-1} \quad (16)$$

A tentative plot of g according to Equations (14) and (16) and the exchange curve of Figure 4 is given together with Z in Figure 5, in which the central horizontal dotted portion of the curve corresponds to the particular value $M_{KBr,I-II} = 0.32$ which is a constant from $N_{Or,I}$ to $N_{Or,II}$.

Substituting Equations (12), (13), and (14) in Equation (11), the condition for exchange equilibrium results in the following condensed relation:

$$\frac{\partial \bar{G}_i^{\text{ex}}(N_{Or})}{\partial N_{Or}} = -C + Z(N_{Or}) + g(N_{Or}) \quad (17)$$

Integration of Basic Equation

The problem of integrating the fundamental relation Equation (17) is more complex than in our previous work (Delbove, 1971), due to the miscibility gap occurring between $N_{Or,I}$ and $N_{Or,II}$.

$\bar{G}_i^{\text{ex}}(N_{Or})$ is known already to equal zero at both extremities (0,1) of the composition range, so we can write for the interval $0 \leq N_{Or} \leq N_{Or,I}$:

$$\bar{G}_i^{\text{ex}}(N_{Or}) = -CN_{Or} + \int_0^{N_{Or}} Z(N_{Or}) dN_{Or} + \int_0^{N_{Or}} g(N_{Or}) dN_{Or} \quad (18)$$

and for the interval $N_{Or,II} \leq N_{Or} \leq 1$:

$$\bar{G}_i^{\text{ex}}(N_{Or}) = +C(1 - N_{Or}) - \int_{N_{Or}}^1 Z(N_{Or}) dN_{Or} - \int_{N_{Or}}^1 g(N_{Or}) dN_{Or} \quad (19)$$

with Z and g being perfectly well-defined and single-valued functions of feldspar composition. The problem of calculating $\bar{G}_f^{\text{ex}}(N_{\text{Or}})$ reduces, therefore, to determine the constant C .

Derivation of the Constant C: Utilization of Combined Exchange and Two-Feldspar Data

Thompson and Waldbaum (1968) give a good account of the problem of equilibrium in two-feldspar assemblages, distinguishing the case with only partial ion-exchange equilibrium, for which

$$\begin{aligned} [\mu_{\text{Or}} - \mu_{\text{Ab}}]_{f, N_{\text{Or}, I}} &= [\mu_{\text{Or}} - \mu_{\text{Ab}}]_{f, N_{\text{Or}, II}} \\ &= [\mu_{\text{KBr}} - \mu_{\text{NaBr}}]_{g, M_{\text{KBr}, I-II}}, \end{aligned} \quad (20)$$

from that with complete equilibrium, that is, that for which the supplementary relations

$$\mu_{\text{Or}}(N_{\text{Or}, I}) = \mu_{\text{Or}}(N_{\text{Or}, II}) \quad (21)$$

$$\mu_{\text{Ab}}(N_{\text{Or}, I}) = \mu_{\text{Ab}}(N_{\text{Or}, II}) \quad (21')$$

are to be added. In the latter case, as illustrated by Thompson and Waldbaum (their Fig. 1b), tangents to the \bar{G}_f curve, at points corresponding to abscissa $N_{\text{Or}, I}$ and $N_{\text{Or}, II}$ (their points a and b), are on the same straight line. The slope of this line, besides, is the same as that of the tangent to \bar{G}_s curve at the point corresponding to the abscissa of $M_{\text{KBr}, I-II}$ (their point f). The validity of the following treatment rests essentially on such a complete equilibrium having been attained, that is, $N_{\text{Or}, I}$ and $N_{\text{Or}, II}$ being true binodal compositions.

The relation between the \bar{G}_f values at the two binodal compositions, $N_{\text{Or}, I}$ and $N_{\text{Or}, II}$, may then be expressed as:

$$\begin{aligned} \bar{G}_f(N_{\text{Or}, II}) - \bar{G}_f(N_{\text{Or}, I}) &= (N_{\text{Or}, II} - N_{\text{Or}, I}) \left[\frac{\partial \bar{G}_f(N_{\text{Or}, I})}{\partial N_{\text{Or}}} \right] \end{aligned} \quad (22)$$

which, due to the ion exchange equilibrium with fused salt, can be converted into:

$$\begin{aligned} \bar{G}_f(N_{\text{Or}, II}) - \bar{G}_f(N_{\text{Or}, I}) &= (N_{\text{Or}, II} - N_{\text{Or}, I}) \left[\frac{\partial \bar{G}_s(M_{\text{KBr}, I-II})}{\partial M_{\text{KBr}}} \right] \end{aligned} \quad (23)$$

The latter equation may be modified as follows. The left-hand side can be shown to be (see Appendix 1)

$$\begin{aligned} \bar{G}_f(N_{\text{Or}, II}) - \bar{G}_f(N_{\text{Or}, I}) &= (N_{\text{Or}, II} - N_{\text{Or}, I})(G_{\text{Or}}^{\circ} - G_{\text{Ab}}^{\circ}) \\ &+ RT \int_{N_{\text{Or}, I}}^{N_{\text{Or}, II}} \ln \frac{N}{1-N} dN \\ &+ \bar{G}_f^{\text{ex}}(N_{\text{Or}, II}) - \bar{G}_f^{\text{ex}}(N_{\text{Or}, I}) \end{aligned} \quad (24)$$

Substitution of Equations (4) and (5) on the right-

hand side gives

$$\begin{aligned} (N_{\text{Or}, II} - N_{\text{Or}, I}) &\left[\frac{\partial \bar{G}_s(M_{\text{KBr}, I-II})}{\partial M_{\text{KBr}}} \right] \\ &= (N_{\text{Or}, II} - N_{\text{Or}, I}) \left[(G_{\text{KBr}}^{\circ} - G_{\text{NaBr}}^{\circ}) \right. \\ &\left. + RT \ln \frac{M_{\text{KBr}, I-II}}{M_{\text{NaBr}, I-II}} + \frac{\partial \bar{G}_s^{\text{ex}}(M_{\text{KBr}, I-II})}{\partial M_{\text{KBr}}} \right] \end{aligned} \quad (25)$$

Combining Equations (24) and (25), and putting the \bar{G}_f^{ex} terms on the left, we obtain

$$\begin{aligned} \bar{G}_f^{\text{ex}}(N_{\text{Or}, II}) - \bar{G}_f^{\text{ex}}(N_{\text{Or}, I}) &= -(N_{\text{Or}, II} - N_{\text{Or}, I}) \\ &\cdot [(G_{\text{Or}}^{\circ} - G_{\text{Ab}}^{\circ}) - (G_{\text{KBr}}^{\circ} - G_{\text{NaBr}}^{\circ})] \\ &- RT \int_{N_{\text{Or}, I}}^{N_{\text{Or}, II}} \ln \frac{N(1 - M_{\text{KBr}, I-II})}{(1 - N)M_{\text{KBr}, I-II}} dN \\ &+ (N_{\text{Or}, II} - N_{\text{Or}, I}) \left[\frac{\partial \bar{G}_s^{\text{ex}}(M_{\text{KBr}, I-II})}{\partial M_{\text{KBr}}} \right] \end{aligned} \quad (26)$$

Equation (26) can be simplified by observing that the bracketed quantity in the first term on the right-hand side equals the constant C , as defined by Equation (12), and that the logarithmic expression under the integral is $Z(N_{\text{Or}})$ as defined by Equation (13), if N_{Or} is assumed to vary continuously from $N_{\text{Or}, I}$ to $N_{\text{Or}, II}$ whereas M_{KBr} remains at the constant value $M_{\text{KBr}, I-II}$. The dotted central portion of curve Z in Figure 5 denotes these special values of $Z(N_{\text{Or}})$. The derivative of \bar{G}_s^{ex} for the special value $M_{\text{KBr}, I-II}$ is a constant. So, from Equation (14), it may be replaced by the function $g(N_{\text{Or}})$, which is constant in the interval $N_{\text{Or}, I} - N_{\text{Or}, II}$, as represented by the dotted horizontal line in Figure 5.

These observations lead to the following condensed expression for Equation (26):

$$\begin{aligned} \bar{G}_f^{\text{ex}}(N_{\text{Or}, II}) - \bar{G}_f^{\text{ex}}(N_{\text{Or}, I}) &= -C(N_{\text{Or}, II} - N_{\text{Or}, I}) \\ &+ \int_{N_{\text{Or}, I}}^{N_{\text{Or}, II}} Z(N_{\text{Or}}) dN_{\text{Or}} \\ &+ \int_{N_{\text{Or}, I}}^{N_{\text{Or}, II}} g(N_{\text{Or}}) dN_{\text{Or}} \end{aligned} \quad (27)$$

Turning to the values of $\bar{G}_f^{\text{ex}}(N_{\text{Or}, I})$ and $\bar{G}_f^{\text{ex}}(N_{\text{Or}, II})$ which, according to Equations (18) and (19), are given by

$$\begin{aligned} \bar{G}_f^{\text{ex}}(N_{\text{Or}, I}) &= -CN_{\text{Or}, I} \\ &+ \int_0^{N_{\text{Or}, I}} Z(N_{\text{Or}}) dN_{\text{Or}} + \int_0^{N_{\text{Or}, I}} g(N_{\text{Or}}) dN_{\text{Or}} \end{aligned} \quad (28)$$

$$\begin{aligned} -\bar{G}_f^{\text{ex}}(N_{\text{Or}, II}) &= -C(1 - N_{\text{Or}, II}) \\ &+ \int_{N_{\text{Or}, II}}^1 Z(N_{\text{Or}}) dN_{\text{Or}} + \int_{N_{\text{Or}, II}}^1 g(N_{\text{Or}}) dN_{\text{Or}} \end{aligned} \quad (29)$$

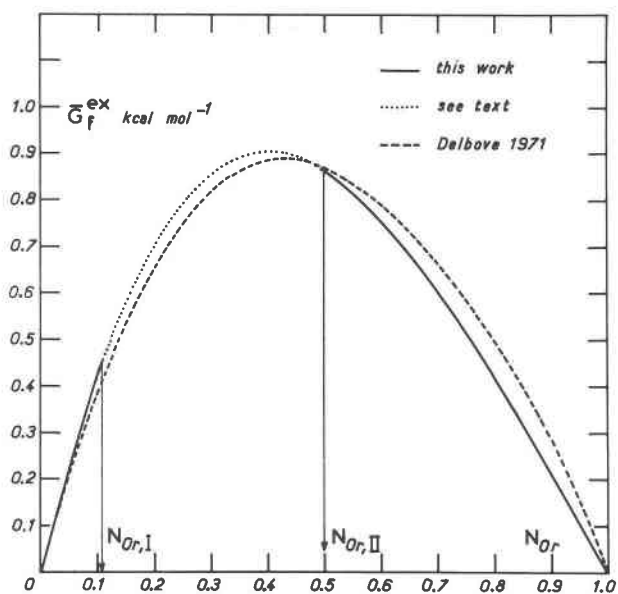


FIG. 6. Excess Gibbs energy, $\bar{G}_f^{\text{ex}}(N_{\text{Or}})$, of highly-ordered alkali feldspars at 800°C and 1 bar (solid curve), calculated from integration of Z and g as plotted in Figure 5. The dotted central portion corresponds to integration being pursued along the dotted paths in Figure 5. The dashed curve is for synthetic disordered alkali feldspars (Delbove, 1971).

we obtain, finally, after combining Equations (27), (28), and (29)

$$C = \int_0^{N_{\text{Or},\text{I}}} (Z + g) dN_{\text{Or}} + \int_{N_{\text{Or},\text{I}}}^{N_{\text{Or},\text{II}}} (Z + g) dN_{\text{Or}} + \int_{N_{\text{Or},\text{II}}}^1 (Z + g) dN_{\text{Or}} \quad (30)$$

Equation (30) shows that C is to be calculated in the same way as would be the case with but one feldspar occurring in the whole range of concentration, C being then given by:

$$C = \int_0^1 (Z + g) dN_{\text{Or}} \quad (31)$$

In terms of graphical treatment based upon an exchange curve like that of Figure 4, it means that the dotted vertical line, which accounts for the miscibility gap between $N_{\text{Or},\text{I}}$ and $N_{\text{Or},\text{II}}$, may be treated as though it were a continuous vertical exchange path.

Results and Discussion

Integration of Z and g , as plotted in Figure 5, gives, according to Equation (30),

$$C = -965 \text{ cal mol}^{-1}.$$

The Janaf *Thermochemical Tables* (1965, 1967) give

$-5970 \text{ cal mol}^{-1}$ for the difference ($G_{\text{KBr}}^{\circ} - G_{\text{NaBr}}^{\circ}$) at 800°C. From Equation (12) we then calculate the difference ($G_{\text{Or}}^{\circ} - G_{\text{Ab}}^{\circ}$) to be $-6935 \text{ cal mol}^{-1}$ compared to $-7560 \text{ cal mol}^{-1}$ as given by Robie and Waldbaum (1968).

A plot of calculated \bar{G}_f^{ex} according to Equations (18) and (19) is given in Figure 6 against N_{Or} . \bar{G}_f^{ex} is, in fact, undetermined in the two-feldspar region; the dotted portion of the curve corresponding to this region has no actual significance as to \bar{G}_f^{ex} of hypothetical feldspars of these intermediate compositions. Simply, it is the result of integrating on Z and g beyond $N_{\text{Or},\text{I}} = 0.105$, taking into account the dotted portions of the Z and g curves in Figure 5, this procedure being merely a mathematical means of connecting $\bar{G}_f^{\text{ex}}(N_{\text{Or},\text{II}})$ to $\bar{G}_f^{\text{ex}}(N_{\text{Or},\text{I}})$. Those values of \bar{G}_f^{ex} are in fact the minimum possible and, if added to \bar{G}_f^{id} , give \bar{G}_f^{t} values that vary along a straight line in the two-feldspar region (see Appendix B for a more complete discussion).

The plot of \bar{G}_f^{ex} for sanidine-high albite feldspars as obtained in our previous study (Delbove, 1971) is also represented in Figure 6 as a dashed curve, the maximum of which is nearly equal to that for ordered feldspars (about 900 cal mol⁻¹). However, \bar{G}_f^{ex} of ordered feldspar is characterized by a greater asymmetry towards NaAlSi₃O₈.

The ion-exchange data of Orville (1963) led Thompson and Waldbaum (1968) to a polythermal Margules-type formula (Eq. 39) for \bar{G}_f^{ex} of sanidine-high albite feldspars (see also Thompson and Waldbaum, 1969b). In another way, their two-phase data led Bachinski and Müller (1971 p. 347) to a similar formula for \bar{G}_f^{ex} of microcline-low albite feldspars. Using these formulae, it is possible to obtain an alternative evaluation of \bar{G}_f^{ex} of both feldspar series at 800°C.

With the purpose of comparing all these data with ours, we can use the $\bar{G}_f^{\text{ex}}/(N_{\text{Or}}N_{\text{Ab}})$ function as the best means of representing the characteristic features of each of them. This has been plotted in Figure 7.

If we approximate \bar{G}_f^{ex} by an asymmetric Margules-type equation with only two parameters, $W_{G,\text{Or}}$ and $W_{G,\text{Ab}}$, then the above-mentioned function is depicted by a straight line, the equation of which is $\bar{G}_f^{\text{ex}}/(N_{\text{Or}}N_{\text{Ab}}) = W_{G,\text{Or}}N_{\text{Ab}} + W_{G,\text{Ab}}N_{\text{Or}}$. The greater the difference of the W_G 's, the greater the slope of this line and the greater the asymmetry of the \bar{G}_f^{ex} curve. From Figure 7 it appears that the $W_{G,\text{Or}}$'s would be about the same for both feldspar series (about 4500 – 5000 cal mol⁻¹), while $W_{G,\text{Ab}}$ would be less in the case of ordered feldspars (about 1000 – 2000 cal mol⁻¹)

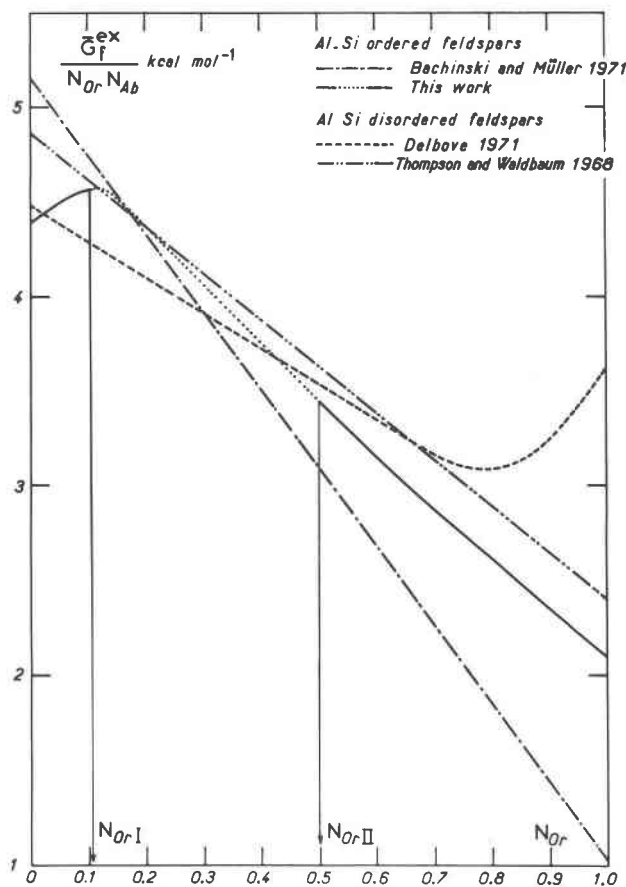


FIG. 7. Plots of $(\bar{G}_f^{\text{ex}}/N_{\text{Or}}N_{\text{Ab}})$ versus N_{Or} at 800°C and 1 bar for Al-Si ordered and disordered alkali feldspars and from different sources of data (see also results of Thompson and Waldbaum, 1969b).

than for disordered feldspars (about 2500 cal mol⁻¹). Now, the significant point to be noted is that unmixing occurs when \bar{G}_f^{ex} is more asymmetric and not necessarily when \bar{G}_f^{ex} is greater in magnitude. This example for feldspars illustrates that mixing properties of solutions are to be accounted for not only in terms of the average magnitude of the excess Gibbs energy (as in the simplest case of regular symmetric solutions), but also by the degree of asymmetry of this function.

Nevertheless, it appears from our curves that $\bar{G}_f^{\text{ex}}/(N_{\text{Or}}N_{\text{Ab}})$ cannot be rigorously approximated by a straight line, for either the ordered or the disordered feldspar. So, it seems necessary to call upon a Margules series development for \bar{G}_f^{ex} with higher power terms, that is, with supplementary excess parameters. In that situation, Williams (1969) showed that analytical representation of excess mixing properties is possible by means of a more suitable

series such as the Fourier Series. \bar{G}_f^{ex} will be expressed as a Fourier Series in the mole fraction N_{Or} :

$$\bar{G}_f^{\text{ex}} = \alpha_1 \sin \pi N_{\text{Or}} + \alpha_2 \sin 2\pi N_{\text{Or}} + \dots + \alpha_i \sin i\pi N_{\text{Or}} \quad (32)$$

in which only sine terms appear, because \bar{G}_f^{ex} equals zero for both $N_{\text{Or}} = 0$ and $N_{\text{Or}} = 1$. The principal advantage of such a series is its orthogonality which results in the $\alpha_1, \alpha_2, \dots, \alpha_i$ parameters being not correlated, as is the case in a Margules-type or equivalent expression. The excess parameters $\alpha_1, \alpha_2, \dots, \alpha_i$ are given by the formula

$$\alpha_i = 2 \int_0^1 \bar{G}_f^{\text{ex}}(N_{\text{Or}}) \sin i\pi N_{\text{Or}} dN_{\text{Or}} \quad (33)$$

The above integrations are possible only if \bar{G}_f^{ex} has definite values in the whole range of concentrations. This means that in the present case of ordered feldspars, because \bar{G}_f^{ex} is in fact undetermined in the two-phase region (the minimum possible values only being known), proper values must be assigned to \bar{G}_f^{ex} in that intermediate range of compositions. Any given assignment will result in a given set of $\alpha_1, \alpha_2, \dots, \alpha_i$ parameters. A particular assignment may be to take as values of \bar{G}_f^{ex} those minimum values as represented by the dotted portion of the curve in Figure 6. The $\alpha_1, \alpha_2, \dots, \alpha_i$ parameters calculated with this assignment are given in Table 4 together with the same parameters for disordered feldspars from our previous study (Delbove, 1971). The greater asymmetry of excess Gibbs energy of ordered feldspars is well marked by the greater relative importance of the $\alpha_2, \alpha_4, \dots$ parameters.

One may now ask what type of influence is exerted on $\alpha_1, \alpha_2, \dots, \alpha_i$ Fourier parameters of ordered feldspars by those minimum dotted values assigned above to \bar{G}_f^{ex} in the two-feldspar region. This can be best answered by considering in Figure 8 plots of μ_{Or} , μ_{Ab} and $\mu_{\text{Or}} - \mu_{\text{Ab}}$ which can be readily derived using the above set of α_i parameters. It may be seen that horizontal straight lines represent these functions within the two-feldspar region, simply as a consequence of \bar{G}_f^{ex} having been assumed to vary according to a straight line. In fact, the later hypothesis is inex-

TABLE 4. Fourier Series Coefficients for \bar{G}_f^{ex} of Al-Si Ordered and Disordered Alkali Feldspar at 800°C, 1 Bar (cal mol⁻¹)

Feldspar	α_1	α_2	α_3	α_4	α_5	α_6	α_7	α_8
Ordered	894	143	36	13	6	4	negl.	negl.
Disordered	920	83	55	6	13	4	12	negl.

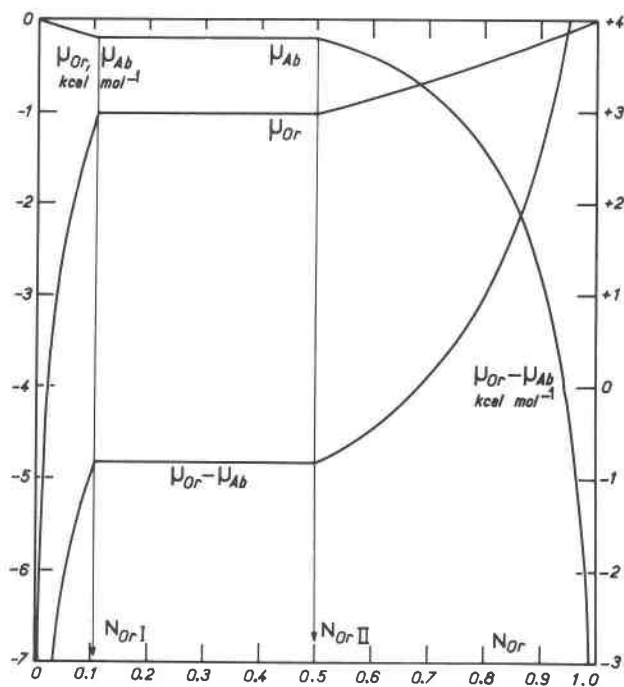


FIG. 8. Plots of μ_{Or} , μ_{Ab} and $\mu_{Or} - \mu_{Ab}$ versus N_{Or} using Fourier series excess parameters as given in Table 4, this paper, for highly-ordered alkali feldspars (G°_{Or} and G°_{Ab} are omitted in the expression of these quantities as given by Equations 1 and 1').

act and the horizontal straight lines must be sinuous curves with a maximum and a minimum (for the "spinodal" compositions); for instance, considering $\mu_{Or} - \mu_{Ab}$, the "equal areas" condition specifies that our horizontal straight line divides the undetermined corresponding sinuous curve into two portions of equal and opposite areas (Waldbaum and Thompson, 1969, Figure 4). Nevertheless, as evidenced by Equations (18), (19), and (30), in spite of this inexact hypothesis as for the two-phase region, the correctness of the calculation of \bar{G}_f^{ex} (and of the derivative functions) in the one-phase region is perfectly well established. Then, a plot of $(\mu_{Or} - \mu_{Ab})$ obeying the "equal areas" condition within the two-phase region, while remaining identical to that of Figure 8 in the one-phase region, is to be obtained by adding extra parameters $\alpha'_1, \alpha'_2, \dots, \alpha'_i, \dots$ to the primitive set of $\alpha_1, \alpha_2, \dots, \alpha_i$ parameters. These α'_i must satisfy the obvious conditions:

$$\left. \begin{aligned} \sum_i \alpha'_i \cos(i\pi N_{Or}) &= 0 \\ \sum_i \alpha'_i \sin(i\pi N_{Or}) &= 0 \end{aligned} \right\} \begin{aligned} &\text{for } 0 \leq N_{Or} \leq N_{Or,I} \\ &\text{and } N_{Or,II} \leq N_{Or} \leq 1 \end{aligned} \quad (32)$$

$$\sum_i \alpha'_i \sin(i\pi N_{Or}) > 0$$

for $N_{Or,I} < N_{Or} < N_{Or,II}$ (33)

and

$$\int_{N_{Or,I}}^{N_{Or,II}} \alpha'_i \cos(i\pi N_{Or}) dN_{Or} = 0 \quad (34)$$

It may be shown that many sets of α'_i parameters will satisfy the relations Equations (32) to (34).

Thus, we are in the peculiar situation of having a Fourier Series based on a particular set of $\alpha_1, \alpha_2, \dots, \alpha_i$ parameters and providing a perfectly good representation of excess Gibbs energy everywhere except inside the miscibility gap, due to those α_i parameters not being single-valued and being in fact erroneous by an underdetermined amount.

Considering now the asymmetric \bar{G}_f^{ex} curve as a whole, it is interesting to have an estimate of what part is due to excess enthalpy and what part to excess entropy. The enthalpy \bar{H}_f^{ex} , may be estimated from calorimetric data at 50°C of Waldbaum and Robie (1971), or from the two-phase data of Bachinski and Müller (1971). Whatever set of these data is chosen, \bar{H}_f^{ex} obviously appears to be much greater than \bar{G}_f^{ex} (the maximum value of \bar{H}_f^{ex} is about 2 times as great as that of \bar{G}_f^{ex}), but less asymmetric. So, it is necessary to assume relatively large and very asymmetric excess positive entropy, with \bar{S}_f^{ex} being much larger on the Or side than on the Ab side. This assumption agrees well with the values of 2.17 cal K⁻¹ mol⁻¹ for $W_{S,Or}$ and 6.48 cal K⁻¹ mol⁻¹ for $W_{S,Ab}$ that were calculated by Bachinski and Müller from their polythermal two-phase study. The origin of such an excess positive entropy may be attributed to multiple causes. Following Thompson and Waldbaum (1969a) and Waldbaum and Robie (1971), excess vibrational entropy may be put forward, but according to Green (1970) that is not sufficient, and configurational excess entropy must be the principal cause, which requires the incorporation of vacancies and other defects in the crystal. With Green's hypothesis and \bar{S}_f^{ex} being greater at the Or-side, it would mean that more vacancies are to be created in a K-rich feldspar than in an Na-rich one, which would be somewhat surprising, the opposite situation being more likely.

Conclusions

The main result of this study is that the excess Gibbs energy \bar{G}_f^{ex} of any binary solution, even with a miscibility gap, can be derived from appropriate ion-exchange experiments. In the present case of highly-ordered feldspars, the use of fused salts instead of hydrothermal salt solutions is the only method possible. The lack of data concerning the excess mixing properties of fused salt systems is not a major in-

convenience, since these quantities are relatively low-valued with respect to those of minerals of interest. Nevertheless, more data in a greater range of temperature and pressure would be very valuable and would permit further extension of this work.

The excess Gibbs energy of low albite-microcline feldspars is positive and not very different from that for high albite-sanidine feldspars, but more asymmetric. The major contribution to the positive value is enthalpic, whereas entropy appears to be responsible for the asymmetry. Crystallographic investigation of Na-K mixing seems necessary to fully understand these results.

Finally, studies on glasses of feldspar composition seem most desirable. From results of Chenebaux (1960) on natural mineral glasses and Garfinkel (1968) on silicate industrial glasses (see Waldbaum and Thompson, 1969, for results on feldspar glasses), a negative excess Gibbs energy is to be expected.

Appendix

A. Calculation of $\bar{G}_f(N_{Or,II}) - \bar{G}_f(N_{Or,I})$

Using the expanded formulation for $\bar{G}_f(N_{Or})$ as given by Equation 2, we obtain for the above difference:

$$\bar{G}_f(N_{Or,II}) - \bar{G}_f(N_{Or,I}) = \begin{cases} (N_{Or,II} - N_{Or,I})(G_{Or}^0 - G_{Ab}^0) \\ + RT[N_{Or,II} \ln N_{Or,II} + (1 - N_{Or,II}) \\ \cdot \ln(1 - N_{Or,II}) - N_{Or,I} \ln N_{Or,I} \\ - (1 - N_{Or,I}) \ln(1 - N_{Or,I})] \\ + \bar{G}_f^{ex}(N_{Or,II}) - \bar{G}_f^{ex}(N_{Or,I}) \end{cases} \quad (A-1)$$

The bracketed quantity may be made simpler by considering the relation $\int \ln N \, dN = N \ln N - N$; we have

$$\begin{aligned} & [N_{Or,II} \ln N_{Or,II} - N_{Or,I} \ln N_{Or,I} + (1 - N_{Or,II}) \\ & \cdot \ln(1 - N_{Or,II}) - (1 - N_{Or,I}) \ln(1 - N_{Or,I})] \\ & = [N_{Or,II} \ln N_{Or,II} - N_{Or,II} - N_{Or,I} \\ & \cdot \ln N_{Or,I} + N_{Or,I}] + [(1 - N_{Or,II}) \\ & \cdot \ln(1 - N_{Or,II}) - (1 - N_{Or,II}) - (1 - N_{Or,I}) \\ & \cdot \ln(1 - N_{Or,I}) + (1 - N_{Or,I})] \\ & = \int_{N_{Or,I}}^{N_{Or,II}} \ln N \, dN + \int_{1-N_{Or,I}}^{1-N_{Or,II}} \ln(1 - N) \\ & \cdot d(1 - N) = \int_{N_{Or,I}}^{N_{Or,II}} \ln \frac{N}{1 - N} \, dN \end{aligned} \quad (A-2)$$

B. Why is the slope of the Z curve in Figure 5 discontinuous at the binodal compositions?

To consider why the slope of the Z curve in Figure 5 is discontinuous at the binodal compositions, we differentiate Equation (17) to obtain

$$\frac{d^2 \bar{G}_f^{ex}}{dN_{Or}^2} = \frac{dZ}{dN_{Or}} + \frac{dg}{dN_{Or}} \quad (B-1)$$

As a particular case and in order to simplify things, we can assume the molten binary salt to be ideal that is: $g = 0$ and $dg/dN_{Or} = 0$ in the whole range of compositions. Then Eq. B-1 reduces to:

$$\frac{d^2 \bar{G}_f^{ex}}{dN_{Or}^2} = \frac{dZ}{dN_{Or}} \quad (B-2)$$

So, a discontinuity of the first derivative of Z is to be related to a discontinuity of the second derivative of \bar{G}_f^{ex} .

Let us consider now \bar{G}_f^t , the total Gibbs energy as plotted in Figure 1b of Thompson and Waldbaum (1968). Occurrence of unmixing is normally expressed by the undetermined sinuous central portion of the curve between a and b. In our treatment, as expressed by Equation (23), where $N_{Or,I}$ and $N_{Or,II}$ stand for the abscissa of a and b and $M_{KBr, I-II}$ for the abscissa of f, we replace this undetermined sinuous portion by the linear segment ab, which leads us to assume

$$\frac{d\bar{G}_f^t}{dN_{Or}} = \text{Cte, and so:} \quad (B-3)$$

$$\frac{d^2 \bar{G}_f^t}{dN_{Or}^2} = 0 \quad (B-4)$$

In fact, $(d^2 \bar{G}_f^t / dN_{Or}^2)$ is positive in the one-phase region and is normally so in the two-phase region except at the spinodal points, where it cancels out, and between them, where it is negative. So, our treatment makes the value of $(d^2 \bar{G}_f^t / dN_{Or}^2)$ vanish suddenly when passing through the binodal points.

Now, the relation

$$\frac{d^2 \bar{G}_f^t}{dN_{Or}^2} = \frac{RT}{N_{Or} N_{Ab}} + \frac{d^2 \bar{G}_f^{ex}}{dN_{Or}^2}, \quad (B-5)$$

in which $RT/(N_{Or} N_{Ab})$ is a continuous function of N_{Or} , shows that a discontinuity of the second derivative of \bar{G}_f^t should result from a discontinuity of the second derivative of \bar{G}_f^{ex} .

If so, according to Equation (B-2), the slope of Z must be discontinuous at the binodal points.

Acknowledgments

I am grateful to the late Professor D. R. Waldbaum who thoroughly reviewed the first manuscript and kindly provided

me with the computer program for the refinement of unit-cell dimensions. I would like to thank Professor G. Sabatier who initially suggested this work and provided advice and suggestions as work proceeded. Thanks are also due to Dr. J. T. Iiyama for helpful discussions and valuable aid.

References

- BACHINSKI, S. W., AND G. MÜLLER (1971) Experimental determinations of the microcline-low albite solvus. *J. Petrol.* **12**, 329-356.
- BEARDEN, J. A. (1967) X-ray wavelengths. *Rev. Mod. Phys.* **39**, 78-124 [Reprinted as National Standard Reference Data Series. *Natl. Bur. Stand.* **14** (1967)].
- BURNHAM, C. W. (1962) Lattice constant refinement. *Carnegie Inst. Wash. Year Book*, **61**, 132-135.
- CHENEBAUX, J. (1960) Reactions d'échange des ions alcalins dans les verres granitiques: obsidiennes et réinites. *C. R. Acad. Sci. (Paris)*, **250**, 1046-1048.
- DELBOVE, F. (1971) Equilibre d'échange d'ions entre feldspaths alcalins et halogénures sodi-potassiques fondus. Application au calcul des propriétés thermodynamiques de la série des feldspaths alcalins. *Bull. Soc. franc. Minéral. Cristallogr.* **94**, 456-466.
- GARFINKEL, H. M. (1968) Ion-exchange equilibria between glass and molten salts. *J. Phys. Chem.* **72**, 4175-4181.
- GREEN, E. J. (1970) On the perils of thermodynamic modelling. *Geochim. Cosmochim. Acta*, **34**, 1029-1033.
- GUION, J., M. BLANDER, D. HENGSTENBERG, AND K. HAGEMARK (1968) Thermodynamic treatment and electromotive force measurements of the ternary molten salt systems Silver Chloride-Sodium Chloride-Potassium Chloride and Silver Chloride-Sodium Chloride-Cesium Chloride. *J. Phys. Chem.* **72**, 2086-2095.
- HERSH, L. S., AND O. J. KLEPPA (1965) Enthalpies of mixing in some binary liquid halide mixtures. *J. Chem. Phys.* **42**, 1309-1322.
- JANAF (1965, 1967). *Thermochemical Tables*.
- KROLL, H. (1973) Estimation of the Al,Si distribution of feldspars from the lattice translations Tr [110] and Tr [110̄] I. Alkali feldspars. *Contrib. Mineral. Petrol.* **39**, 141-156.
- ORVILLE, P. M. (1963) Alkali ion-exchange between vapor and feldspar phases. *Am. J. Sci.* **261**, 201-237.
- (1967) Unit cell parameters of the microcline-low albite and the sanidine-high albite solid solution series. *Am. Mineral.* **52**, 55-86.
- REISS, H., J. L. KATZ, AND O. J. KLEPPA (1962) Theory of the heats of mixing of certain fused salts. *J. Chem. Phys.* **36**, 144-148.
- ROBIE, R. A., AND D. R. WALDBAUM (1968) Thermodynamic properties of minerals and related substances at 298.15°K (25.01°C) and one atmosphere (1.013 bars) pressure and at higher temperature. *U.S. Geol. Surv. Bull.* **1259**.
- STEWART, D. B., AND P. H. RIBBE (1969) Structural explanation for variations in cell parameters of alkali feldspar with Al/Si ordering. *Am. J. Sci.* **267-A**, 444-462.
- , AND T. L. WRIGHT (1974) Al-Si order and symmetry of natural potassic feldspars, and the relationship of strained cell parameter to bulk composition. *Bull. Soc. franc. Minéral. Cristallogr.* **97**, 356-377.
- THOMPSON, J. B., AND D. R. WALDBAUM (1968) Mixing properties of sanidine crystalline solutions: I. Calculations based on ion-exchange data. *Am. Mineral.* **53**, 1965-1999.
- , AND ——— (1969a) Analysis of the two-phase region halite-sylvite in the system NaCl-KCl. *Geochim. Cosmochim. Acta*, **33**, 671-690.
- , AND ——— (1969b) Mixing properties of sanidine crystalline solutions: III. Calculations based on two-phase data. *Am. Mineral.* **54**, 811-837.
- WALDBAUM, D. R. (1969) Thermodynamic mixing properties of NaCl-KCl liquids. *Geochim. Cosmochim. Acta*, **33**, 1415-1427.
- , AND R. A. ROBIE (1971) Calorimetric investigation of Na-K mixing and polymorphism in the alkali feldspars. *Z. Kristallogr.* **134**, 381-420.
- , AND J. B. THOMPSON (1969) Mixing properties of sanidine crystalline solutions: IV. Phase diagrams from equations of state. *Am. Mineral.* **54**, 1274-1298.
- WILLIAMS, R. O. (1969) Series representation of thermodynamic functions of binary solutions. *Trans. AIME*, **245**, 2565-2570.
- WRIGHT, T. L., AND D. B. STEWART (1968) X-ray and optical study of alkali feldspar: I. Determination of composition and structural state from refined unit-cell parameters and 2V. *Am. Mineral.*, **53**, 38-87.
- WYART, J., AND G. SABATIER (1956) Transformations mutuelles des feldspaths alcalins. Reproduction du microcline et de l'albite. *Bull. Soc. franc. Minéral. Cristallogr.* **79**, 574-581.

Manuscript received, March 12, 1973; accepted
for publication, August 21, 1974.